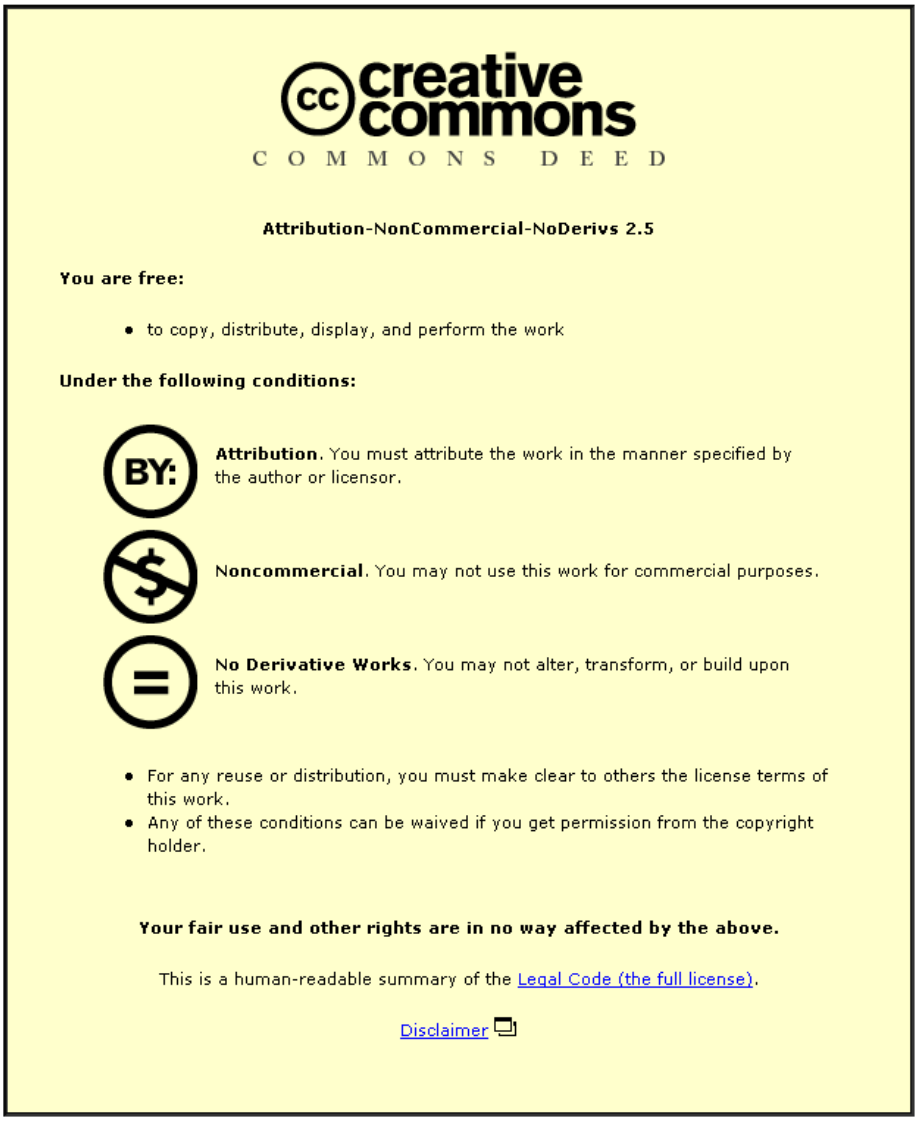

creative commons

COMMONS DEED

Attribution-NonCommercial-NoDerivs 2.5

You are free:

- to copy, distribute, display, and perform the work

Under the following conditions:

Attribution. You must attribute the work in the manner specified by the author or licensor.

Noncommercial. You may not use this work for commercial purposes.

No Derivative Works. You may not alter, transform, or build upon this work.

- For any reuse or distribution, you must make clear to others the license terms of this work.
- Any of these conditions can be waived if you get permission from the copyright holder.

Your fair use and other rights are in no way affected by the above.

This is a human-readable summary of the Legal Code (the full license).

Disclaimer

COMPDYN 2009
ECCOMAS Thematic Conference on
Computational Methods in Structural Dynamics and Earthquake Engineering
M. Papadrakakis, N.D. Lagaros, M. Fragiadakis (eds.)
Rhodes, Greece, 22–24 June 2009

IDENTIFICATION OF DYNAMIC MODELS OF METSOVO (GREECE) BRIDGE USING AMBIENT VIBRATION MEASUREMENTS

Panagiotis Panetsos[1], Evaggelos Ntotsios[2], Nikolaos-Aggelos Liokos[2], Costas Papadimitriou[2]

[1]Egnatia Odos S.A.
Capital Maintenance Department, Thermi 57001, Greece
ppane@egnatia.gr

[2]University of Thessaly
Department of Mechanical Engineering, Volos 38334, Greece
entotsio@uth.gr, nickliokos@yahoo.com, costasp@uth.gr

Keywords: Bridges, Model Updating, Structural Identification, Multi-Objective Optimization, Structural Dynamics.

Abstract. *Available methods for structural model updating are employed to develop high fidelity models of the Metsovo bridge using ambient vibration measurements. The Metsovo bridge, the highest bridge of the Egnatia Odos Motorway, is a two-branch balanced cantilever ravine bridge. It has a total length of 357m, a very long central span of 235m, and a height of 110m for the taller pier. Ambient vibration measurements are available during different construction phases of the bridge. Operational modal analysis software is used to obtain the modal characteristics of the bridge. The modal characteristics are then used to update two model classes of finite element models of the bridge. These model classes are based on beam and solid elements. A multi-objective structural identification method is used for estimating the parameters of the finite element structural models based on minimising the modal residuals. The method results in multiple Pareto optimal structural models that are consistent with the measured modal data and the modal residuals used to measure the discrepancies between the measured modal values and the modal values predicted by the model. Single objective structural identification methods are also evaluated as special cases of the proposed multi-objective identification method. The effectiveness of the updated models from the two model classes and their predictive capabilities are assessed. It is demonstrated that the Pareto optimal structural models may vary considerably, depending on the fidelity of the model classes employed and the size of measurement errors.*

1 INTRODUCTION

Structural model updating methods have been proposed in the past to reconcile mathematical models, usually discretized finite element models, with experimental data. The estimate of the optimal model from a parameterized class of models is sensitive to uncertainties that are due to limitations of the mathematical models used to represent the behavior of the real structure, the presence of measurement and processing error in the data, the number and type of measured modal or response time history data used in the reconciling process, as well as the norms used to measure the fit between measured and model predicted characteristics. The optimal structural models resulting from such methods can be used for improving the model response and reliability predictions [1], structural health monitoring applications [2-5] and structural control [6].

Structural model parameter estimation problems based on measured data, such as modal characteristics (e.g. [2-5]) or response time history characteristics [7], are often formulated as weighted least-squares problems in which metrics, measuring the residuals between measured and model predicted characteristics, are build up into a single weighted residuals metric formed as a weighted average of the multiple individual metrics using weighting factors. Standard optimization techniques are then used to find the optimal values of the structural parameters that minimize the single weighted residuals metric representing an overall measure of fit between measured and model predicted characteristics. Due to model error and measurement noise, the results of the optimization are affected by the values assumed for the weighting factors.

The model updating problem has also been formulated in a multi-objective context [8] that allows the simultaneous minimization of the multiple metrics, eliminating the need for using arbitrary weighting factors for weighting the relative importance of each metric in the overall measure of fit. The multi-objective parameter estimation methodology provides multiple Pareto optimal structural models consistent with the data and the residuals used in the sense that the fit each Pareto optimal model provides in a group of measured modal properties cannot be improved without deteriorating the fit in at least one other modal group.

Theoretical and computational issues arising in multi-objective identification have been addressed and the correspondence between the multi-objective identification and the weighted residuals identification has been established [9-10]. Emphasis was given in addressing issues associated with solving the resulting multi-objective and single-objective optimization problems. For this, efficient methods were also proposed for estimating the gradients and the Hessians [11] of the objective functions using the Nelson's method [12] for finding the sensitivities of the eigenproperties to model parameters.

In this work, the structural model updating problem using modal residuals is formulated as single- and multi-objective optimization problems with the objective formed as a weighted average of the multiple objectives using weighting factors. Theoretical and computational issues are then reviewed and the model updating methodologies are applied to update two different model classes of finite element models of the Metsovo bridge using ambient vibration measurements. Emphasis is given in investigating the variability of the Pareto optimal models from each model class.

2 MODEL UPDATING BASED ON MODAL RESIDUALS

Let $D=\{\hat{\omega}_r^{(k)},\hat{\underline{\phi}}_r^{(k)}\in R^{N_0},\ r=1,\cdots,m,\ k=1,\cdots,N_D\}$ be the measured modal data from a structure, consisting of modal frequencies $\hat{\omega}_r^{(k)}$ and modeshape components $\hat{\underline{\phi}}_r^{(k)}$ at N_0 measured degrees of freedom (DOF), where m is the number of observed modes and N_D is

the number of modal data sets available. Consider a parameterized class of linear structural models used to model the dynamic behavior of the structure and let $\underline{\theta} \in R^{N_\theta}$ be the set of free structural model parameters to be identified using the measured modal data. The objective in a modal-based structural identification methodology is to estimate the values of the parameter set $\underline{\theta}$ so that the modal data $\{\omega_r(\underline{\theta}),\ \underline{\phi}_r(\underline{\theta}) \in R^{N_d}, r=1,\cdots,m\}$, where N_d is the number of model DOF, predicted by the linear class of models best matches, in some sense, the experimentally obtained modal data in D. For this, let

$$\varepsilon_{\omega_r}(\underline{\theta}) = \frac{\omega_r^2(\underline{\theta}) - \hat{\omega}_r^2}{\hat{\omega}_r^2} \qquad \text{and} \qquad \varepsilon_{\underline{\phi}_r}(\underline{\theta}) = \frac{\left\| \beta_r(\underline{\theta}) L\underline{\phi}_r(\underline{\theta}) - \hat{\underline{\phi}}_r \right\|}{\left\| \hat{\underline{\phi}}_r \right\|} \tag{1}$$

$r=1,\cdots,m$, be the measures of fit or residuals between the measured modal data and the model predicted modal data for the r-th modal frequency and modeshape components, respectively, where $\| \underline{z} \|^2 = \underline{z}^{\mathrm{T}} \underline{z}$ is the usual Euclidean norm, and $\beta_r(\underline{\theta}) = \hat{\underline{\phi}}_r^T L\underline{\phi}(\underline{\theta})_r / \left\| L\underline{\phi}_r(\underline{\theta}) \right\|^2$ is a normalization constant that guaranties that the measured modeshape $\hat{\underline{\phi}}_r$ at the measured DOFs is closest to the model modeshape $\beta_r(\underline{\theta}) L\underline{\phi}_r(\underline{\theta})$ predicted by the particular value of $\underline{\theta}$. The matrix $L \in R^{N_0 \times N_d}$ is an observation matrix comprised of zeros and ones that maps the N_d model DOFs to the N_0 observed DOFs.

In order to proceed with the model updating formulation, the measured modal properties are grouped into two groups [10]. The first group contains the modal frequencies while the second group contains the modeshape components for all modes. For each group, a norm is introduced to measure the residuals of the difference between the measured values of the modal properties involved in the group and the corresponding modal values predicted from the model class for a particular value of the parameter set $\underline{\theta}$. For the first group the measure of fit $J_1(\underline{\theta})$ is selected to represent the difference between the measured and the model predicted frequencies for all modes. For the second group the measure of fit $J_2(\underline{\theta})$ is selected to represents the difference between the measured and the model predicted modeshape components for all modes. Specifically, the two measures of fit are given by

$$J_1(\underline{\theta}) = \sum_{r=1}^{m} \varepsilon_{\omega_r}^2(\underline{\theta}) \qquad \text{and} \qquad J_2(\underline{\theta}) = \sum_{r=1}^{m} \varepsilon_{\underline{\phi}_r}^2(\underline{\theta}) \tag{2}$$

The aforementioned grouping scheme is used in the next subsections for demonstrating the features of the proposed model updating methodologies.

2.1 Multi-objective identification

The problem of identifying the model parameter values $\underline{\theta}$ that minimize the modal or response time history residuals can be formulated as a multi-objective optimization problem stated as follows [8]. Find the values of the structural parameter set $\underline{\theta}$ that simultaneously minimizes the objectives

$$\underline{y} = \underline{J}(\underline{\theta}) = (J_1(\underline{\theta}), J_2(\underline{\theta})) \tag{3}$$

subject to parameter constrains $\underline{\theta}_{low} \le \underline{\theta} \le \underline{\theta}_{upper}$, where $\underline{\theta} = (\theta_1, \cdots, \theta_{N_\theta}) \in \Theta$ is the parameter vector, Θ is the parameter space, $\underline{y} = (y_1, \cdots, y_n) \in Y$ is the objective vector, Y is the objec-

tive space and $\underline{\theta}_{low}$ and $\underline{\theta}_{upper}$ are respectively the lower and upper bounds of the parameter vector . For conflicting objectives $J_1(\underline{\theta})$ and $J_2(\underline{\theta})$ there is no single optimal solution, but rather a set of alternative solutions, known as Pareto optimal solutions, that are optimal in the sense that no other solutions in the parameter space are superior to them when both objectives are considered. The set of objective vectors $\underline{y} = \underline{J}(\underline{\theta})$ corresponding to the set of Pareto optimal solutions $\underline{\theta}$ is called Pareto optimal front. The characteristics of the Pareto solutions are that the residuals cannot be improved in one group without deteriorating the residuals in the other group.

The multiple Pareto optimal solutions are due to modelling and measurement errors. The level of modelling and measurement errors affect the size and the distance from the origin of the Pareto front in the objective space, as well as the variability of the Pareto optimal solutions in the parameter space. The variability of the Pareto optimal solutions also depends on the overall sensitivity of the objective functions or, equivalently, the sensitivity of the modal properties, to model parameter values $\underline{\theta}$. Such variabilities were demonstrated for the case of two-dimensional objective space and one-dimensional parameter space in the work by Christodoulou and Papadimitriou [9].

2.2 Weighted modal residuals identification

The parameter estimation problem is traditionally solved by minimizing the single objective

$$J(\underline{\theta}; \underline{w}) = w_1 J_1(\underline{\theta}) + w_2 J_2(\underline{\theta}) \tag{4}$$

formed from the multiple objectives $J_i(\underline{\theta})$ using the weighting factors $w_i \geq 0$, $i = 1,2$, with $w_1 + w_2 = 1$. The objective function $J(\underline{\theta}; \underline{w})$ represents an overall measure of fit between the measured and the model predicted characteristics. The relative importance of the residual errors in the selection of the optimal model is reflected in the choice of the weights. The results of the identification depend on the weight values used. Conventional weighted least squares methods assume equal weight values, $w_1 = w_2 = 1/2$. This conventional method is referred herein as the equally weighted modal residuals method.

The single objective is computationally attractive since conventional minimization algorithms can be applied to solve the problem. However, a severe drawback of generating Pareto optimal solutions by solving the series of weighted single-objective optimization problems by uniformly varying the values of the weights is that this procedure often results in cluster of points in parts of the Pareto front that fail to provide an adequate representation of the entire Pareto shape. Thus, alternative algorithms dealing directly with the multi-objective optimization problem and generating uniformly spread points along the entire Pareto front should be preferred. Formulating the parameter identification problem as a multi-objective minimization problem, the need for using arbitrary weighting factors for weighting the relative importance of the residuals $J_i(\underline{\theta})$ of a modal group to an overall weighted residuals metric is eliminated. An advantage of the multi-objective identification methodology is that all admissible solutions in the parameter space are obtained. Special algorithms are available for solving the multi-objective optimization problem. Computational algorithms and related issues for solving the single-objective and the multi-objective optimization problems are briefly discussed in the next Section.

3 COMPUTATIONAL ISSUES IN MODEL UPDATING

The proposed single and multi-objective identification problems are solved using available single- and multi-objective optimization algorithms. These algorithms are briefly reviewed and various implementation issues are addressed, including estimation of global optima from multiple local/global ones, as well as convergence problems.

3.1 Single-objective identification

The optimization of $J(\underline{\theta};\underline{w})$ in (4) with respect to $\underline{\theta}$ for given $\underline{w}$ can readily be carried out numerically using any available algorithm for optimizing a nonlinear function of several variables. These single objective optimization problems may involve multiple local/global optima. Conventional gradient-based local optimization algorithms lack reliability in dealing with the estimation of multiple local/global optima observed in structural identification problems [9,13], since convergence to the global optimum is not guaranteed. Evolution strategies (ES) [14] are more appropriate and effective to use in such cases. ES are random search algorithms that explore better the parameter space for detecting the neighborhood of the global optimum, avoiding premature convergence to a local optimum. A disadvantage of ES is their slow convergence at the neighborhood of an optimum since they do not exploit the gradient information. A hybrid optimization algorithm should be used that exploits the advantages of ES and gradient-based methods. Specifically, an evolution strategy is used to explore the parameter space and detect the neighborhood of the global optimum. Then the method switches to a gradient-based algorithm starting with the best estimate obtained from the evolution strategy and using gradient information to accelerate convergence to the global optimum.

3.2 Multi-Objective Identification

The set of Pareto optimal solutions can be obtained using available multi-objective optimization algorithms. Among them, the evolutionary algorithms, such as the strength Pareto evolutionary algorithm [15], are well-suited to solve the multi-objective optimization problem. The strength Pareto evolutionary algorithm, although it does not require gradient information, it has the disadvantage of slow convergence for objective vectors close to the Pareto front [8] and also it does not generate an evenly spread Pareto front, especially for large differences in objective functions.

Another very efficient algorithm for solving the multi-objective optimization problem is the Normal-Boundary Intersection (NBI) method [16]. It produces an evenly spread of points along the Pareto front, even for problems for which the relative scaling of the objectives are vastly different. The NBI optimization method involves the solution of constrained nonlinear optimization problems using available gradient-based constrained optimization methods. The NBI uses the gradient information to accelerate convergence to the Pareto front.

3.3 Computations of gradients

In order to guarantee the convergence of the gradient-based optimization methods for structural models involving a large number of DOFs with several contributing modes, the gradients of the objective functions with respect to the parameter set $\underline{\theta}$ has to be estimated accurately. It has been observed that numerical algorithms such as finite difference methods for gradient evaluation does not guarantee convergence due to the fact that the errors in the numerical estimation may provide the wrong directions in the search space and convergence to the local/global minimum is not achieved, especially for intermediate parameter values in the vicinity of a local/global optimum. Thus, the gradients of the objective functions should

be provided analytically. Moreover, gradient computations with respect to the parameter set using the finite difference method requires the solution of as many eigenvalue problems as the number of parameters.

The gradients of the modal frequencies and modeshapes, required in the estimation of the gradient of $J(\underline{\theta};\underline{w})$ in (4) or the gradients of the objectives $J_i(\underline{\theta})$ in (3) are computed by expressing them exactly in terms of the modal frequencies, modeshapes and the gradients of the structural mass and stiffness matrices with respect to $\underline{\theta}$ using Nelson's method [12]. Special attention is given to the computation of the gradients and the Hessians of the objective functions for the point of view of the reduction of the computational time required. Analytical expressions for the gradient of the modal frequencies and modeshapes are used to overcome the convergence problems. In particular, Nelson's method [12] is used for computing analytically the first derivatives of the eigenvalues and the eigenvectors. The advantage of the Nelson's method compared to other methods is that the gradient of the eigenvalue and the eigenvector of one mode are computed from the eigenvalue and the eigenvector of the same mode and there is no need to know the eigenvalues and the eigenvectors from other modes. For each parameter in the set $\underline{\theta}$ this computation is performed by solving a linear system of the same size as the original system mass and stiffness matrices. Nelson's method has also been extended to compute the second derivatives of the eigenvalues and the eigenvectors.

The formulation for the gradient and the Hessian of the objective functions are presented in references [11, 17]. The computation of the gradients and the Hessian of the objective functions is shown to involve the solution of a single linear system, instead of N_θ linear systems required in usual computations of the gradient and N_θ $N_\theta+1$ linear systems required in the computation of the Hessian. This reduces considerably the computational time, especially as the number of parameters in the set $\underline{\theta}$ increase.

4 APPLICATION TO METSOVO BRIDGE

4.1 Description of Metsovo bridge and instrumentation

The new under construction ravine bridge of Metsovo (Figure 1, November 2008), in section 3.2 (Anthohori tunnel-Anilio tunnel) of Egnatia Motorway, is crossing the deep ravine of Metsovitikos river, 150 m over the riverbed. This is the higher bridge of Egnatia Motorway, with the height of the taller pier M2 equal to 110 m. The total length of the bridge is 357 m. As a consequence of the strong inequality of the heights of the two basic piers of the bridge, M2 and M3 (110 m to 35 m), the very long central span of 235 m, is even longer during construction, as the pier M2 balanced cantilever is 250 m long, due to the eccentrical position of the key segment. The key of the central span is not in midspan due to the different heights of the superstructure at its supports to the adjacent piers (13.0 m in pier M2 and 11.50 m in pier M3) for redistributing mass and load in favor of the short pier M3 and thus relaxing strong structural abnormality. The last was the main reason of this bridge to be designed to resist earthquakes fully elastic (q factor equal to 1). The longitudinal section of the left branch of Metsovo ravine bridge is shown in Figure 2.

The bridge has 4 spans of length 44.78 m /117.87 m /235.00 m/140.00 m and three piers of which M1, 45 m high, supports the boxbeam superstructure through pot bearings (movable in both horizontal directions), while M2, M3 piers connect monolithically to the superstructure. The bridge was being constructed by the balanced cantilever method of construction and according to the constructional phases shown in Figures 3(a) and 3(b). The total width of the deck is 13.95 m, for each carriageway. The superstructure is limited prestressed

of single boxbeam section, of height varying from the maximum 13.5 m in its support to pier M2 to the minimum 4.00 m in key section.

Figure 1: General view of Metsovo ravine bridge.

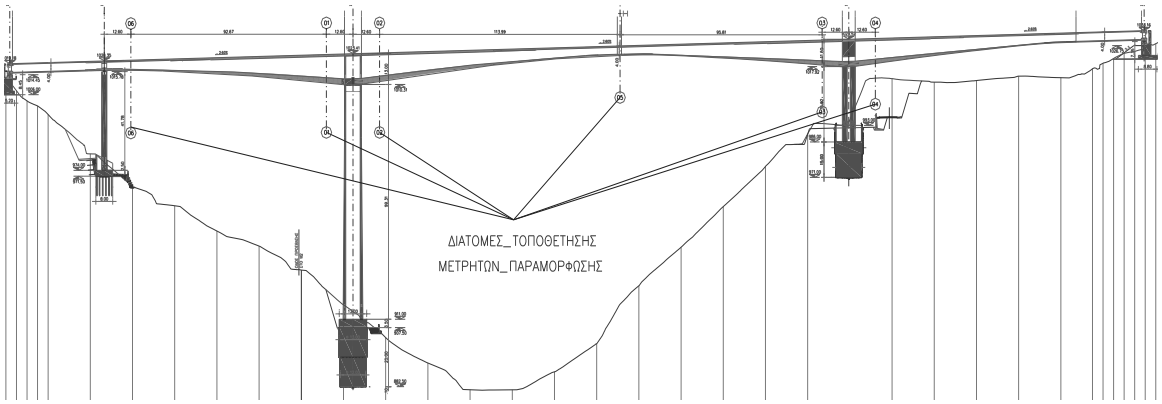

Figure 2: Longitudinal section of Metsovo ravine bridge of Egnatia Motorway.

The pier M3 balanced cantilever was instrumented after the construction of all its segments and before the construction of the key segment that will join with the balanced cantilever of pier M2 (Figure 3). The total length of M3 cantilever was at the time of its instrumentation 215 m while its total height is 35 m. Piers M2, M3 are founded on huge circular Ø12.0 m rock sockets in the steep slopes of the ravine of the Metsovitikos river, in a depth of 25 m and 15 m, respectively.

Figure 3: Views of under construction Metsovo ravine bridge, (a) General view, (b) key of central span.

Six uniaxial accelerometers were installed inside the box beam cantilever M3 of the left carriageway of Metsovo ravine bridge. The accelerometer arrays, are shown in Figure 4. Due to the symmetry of the construction method (balanced cantilevering) and as the same number of segments were completed on both sides of pier M3, the instrumentation was limited to the right cantilever of pier M3, following two basic arrangements. According to the 1st arrangement two (2) sensors were supported on the head of pier M3, one measuring longitudinal and the other transverse accelerations (M3L, M3T), while the remaining four (4) accelerometers were supported on the right and the left internal sides of the box beam's webs , two (2) distant 46m and two (2) distant 68m from M3 axis, respectively (LV3, RV4, LV5, RV6). All four were measuring vertical acceleration. According to the 2nd arrangement the last two sensors of the 1st arrangement were fixed in a section near the cantilever edge, distant 93m from M3 axis, while the other four remain in the same positions. In both arrangements the sixth sensor was adjusted to alternatively measure both in vertical and in transverse horizontal direction (RV6 or RT6).

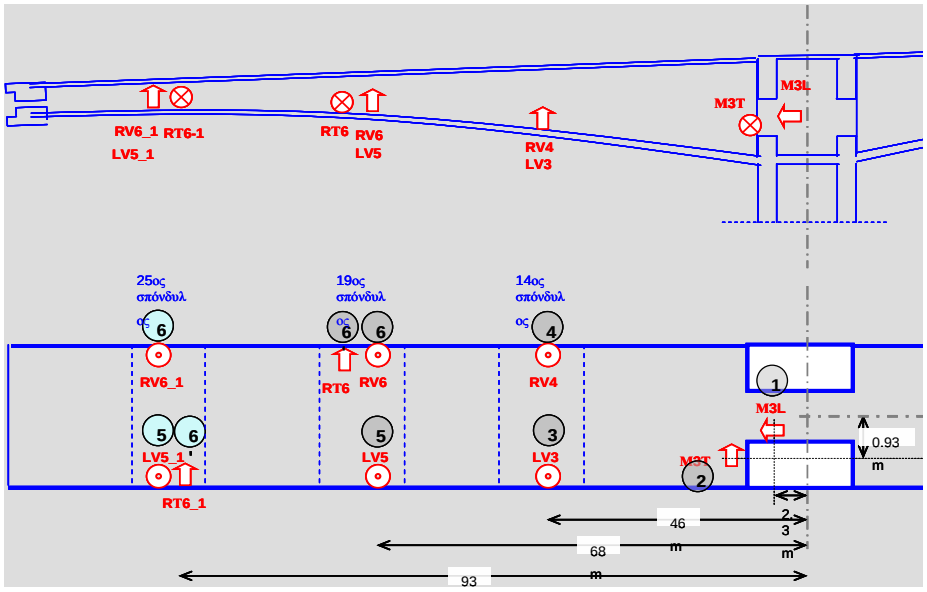

Figure 4: Accelerometer installation arrangements.

4.2 Modal identification

The response of the cantilever structure subjected to ambient loads such as the wind, and loads induced by construction activities such as the crossing of light vehicles placing the prestressing cables inside the tendon tubes, was as expected of very low intensity (0,6% of the acceleration of gravity). From acceleration response time histories, measured from the 6 channel arrays, the cross power spectral density (CPSD) functions were estimated and used to estimate the modal properties using the Modal Identification Toolbox (MITool) [18] developed by the System Dynamics Laboratory in the University of Thessaly. All the basic modal frequencies, modal damping ratios and modeshape components of the bridge were identified.

The identified values of the modal frequencies, their type and the corresponding values of the damping ratios are shown in Table 1. The modal damping ratios reported in Table 1 show that the values of damping are of the order of 0.2% to 2.9%. Due to the small number of available sensors (six) the type of some of the modeshapes were not identified with confidence. The first six identified modeshapes are presented in Figure 5. The arrows are placed in measuring points and their length is proportional to the respective value of the normalized modal component. The accuracy in the estimation of the modal characteristics is shown in Figure 6 comparing the measured with the modal model predicted CPSD. As it is seen, the fit of the measured power spectral density is very good which validates the effectiveness of the proposed modal identification software based on ambient vibrations.

No	Identified Modes	Hz	Damping %	FEM (beam)	FEM (solid)
1	1st rotational, z axis	0.15	2.93	0.15	0.16
2	1st longitudinal	0.30	0.18	0.28	0.29
3	1st transverse	0.62	0.43	0.58	0.61
4	2nd longitudinal	0.68	0.42	0.62	0.66
5	1st bending (deck)	0.90	0.25	0.73	0.97
6	2nd transverse	1.30	0.40	1.30	1.39
7	transverse	1.46	0.47	-	-
8	2nd bending (deck)	2.28	0.47	2.56	2.44
9	2nd rotational, z axis	2.58	0.76	2.07	2.61
10	3rd bending (deck)	3.23	0.40	3.58	3.43
11	3rd transverse	4.63	0.32	3.88	4.61
12	1st rotational, x axis	4.94	0.47	5.72	5.77
13	4th bending (deck)	5.95	1.33	7.12	6.40

Table 1: Identified modes of the Metsovo ravine bridge

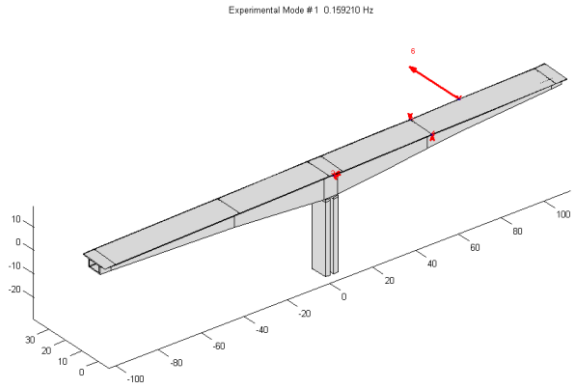
Experimental Mode # 1 0.159210 Hz

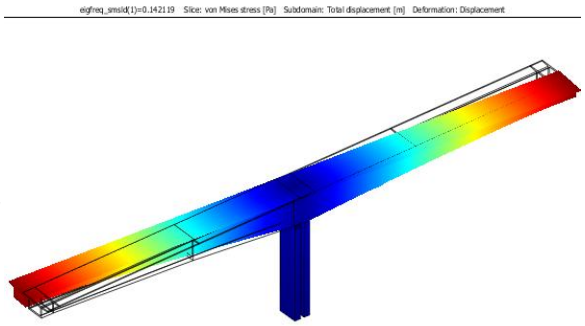
eigfreq_smsld(1)=0.142119 Slice: von Mises stress [Pa] Subdomain: Total displacement [m] Deformation: Displacement

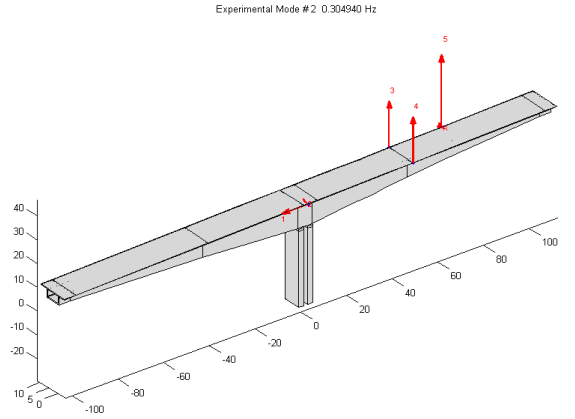
Experimental Mode # 2 0.304940 Hz

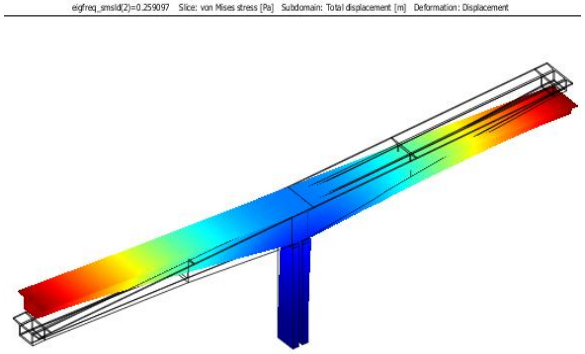
eigfreq_smsld(2)=0.259097 Slice: von Mises stress [Pa] Subdomain: Total displacement [m] Deformation: Displacement

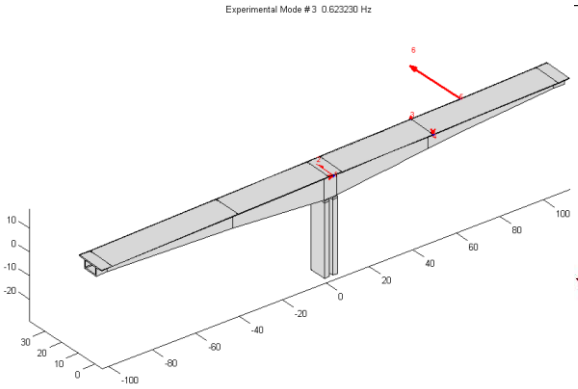
Experimental Mode # 3 0.623230 Hz

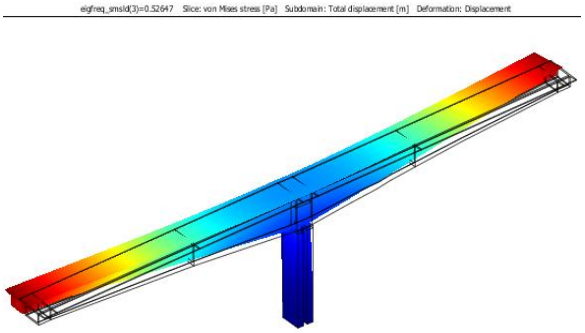
eigfreq_smsld(3)=0.52647 Slice: von Mises stress [Pa] Subdomain: Total displacement [m] Deformation: Displacement

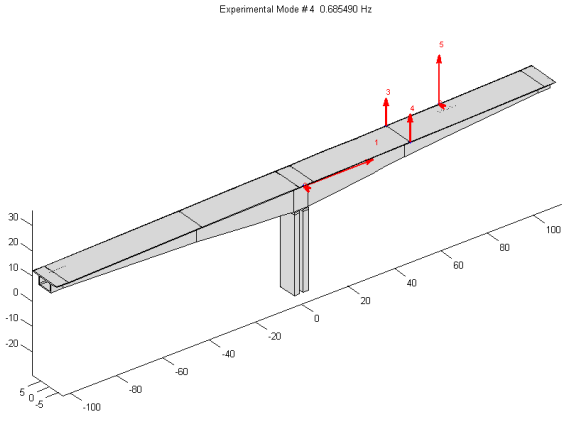
Experimental Mode # 4 0.685490 Hz

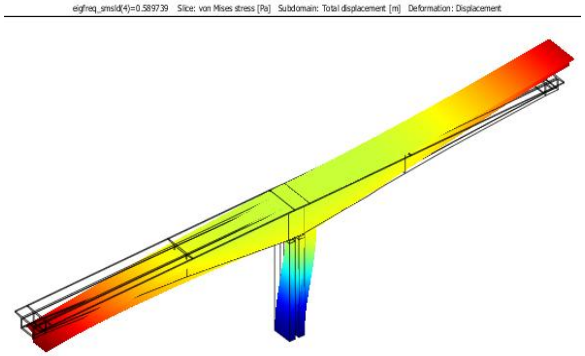
eigfreq_smsld(4)=0.589739 Slice: von Mises stress [Pa] Subdomain: Total displacement [m] Deformation: Displacement

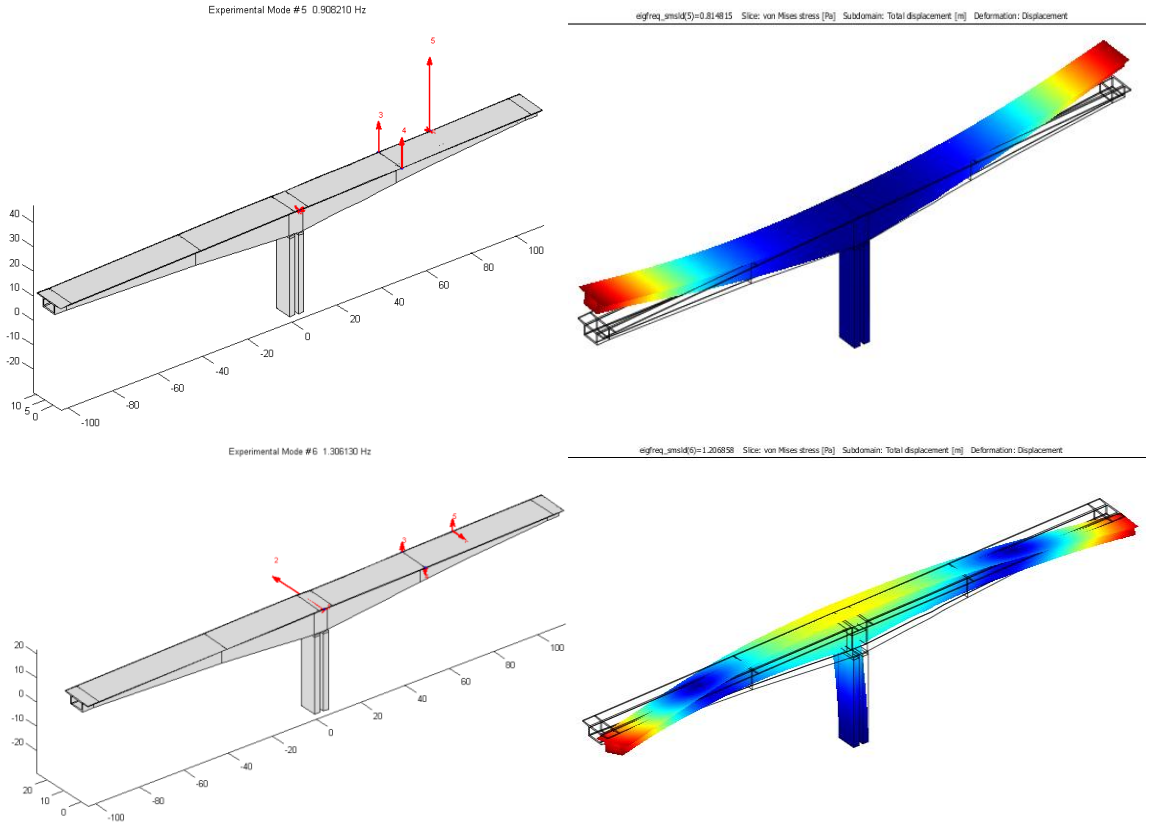

Figure 5: The first six identified modeshapes of Metsovo bridge.

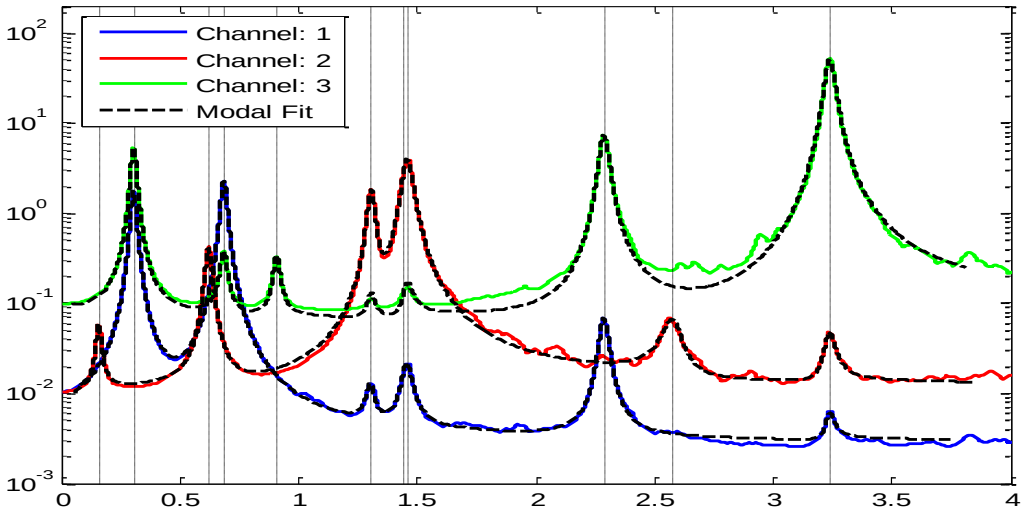

Figure 6: Comparison between measured and modal model predicted CPSD.

4.3 Updating of finite element model classes

Initially, three different analytical dynamic models of the bridge cantilever M3 were constructed, using Euler beam elements representing material and geometry of the structure, as considered by the design. For bridge modeling the software package COMSOL Multiphysics [19] was used. Three dimension Euler beam finite elements were used for the construction of this model, coincided with the axis connecting the centoids of the deck and pier sections. For better graphical representation of the higher modeshapes, on the measured points of the bridge cantilever (positions of sensors), additional rigid transverse extensions of no mass were added to both sides of its centroid axis. For representing rigid connection of the superstructure to the pier, rigid elements of no mass were used. The beam model shown in Figure 7 has 306 degrees of freedom. Pier transverse webs were simulated by beam elements according to design drawings. For comparison purposes, Table 1 lists the values of the modal frequencies predicted by the nominal finite element beam model constructed in the COMSOL Multiphysics software. Comparing with the identified modal frequency values it can be seen that the nominal FEM-based modal frequencies for the beam model are fairly close to the experimental ones.

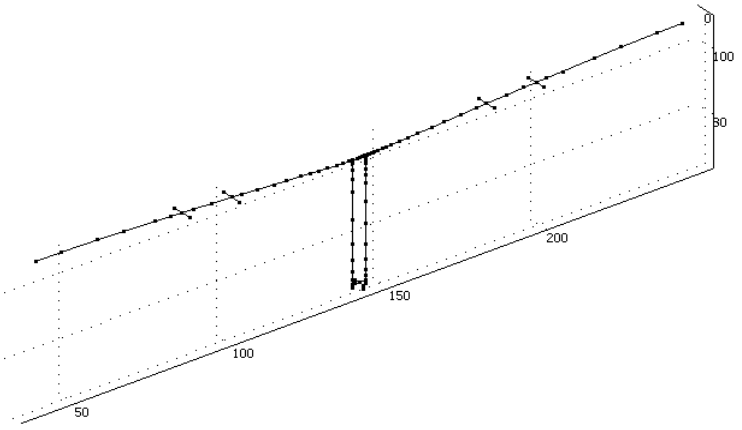

Figure 7: Dynamic model of cantilever M3 of Metsovo bridge with Euler beam finite elements.

Next, detailed finite element models were created using three dimensional solid elements. For this the structure was first designed in CAD environment and then imported in COMSOL Multiphysics [19] modelling environment. The models were constructed based on the material properties and the geometric details of the structure. The finite element models for the bridge were created using three dimensional tetrahedron solid finite elements to model the whole structure. The entire simulation and the model updating is performed within the COMSOL Multiphysics modelling environment using Matlab-based model updating software designed by the System Dynamics Laboratory of the University of Thessaly.

In order to investigate the sensitivity of the model error due to the finite element discretization, several models were created decreasing the size of the elements in the finite element mesh. The resulted twelve finite element models consist of 6683 to 156568 triangular shell elements corresponding to 39291 to 886353 DOF. The convergence in the first six modefrequencies predicted by the finite element models with respect to the number of models DOF is given in Figure 8. According to the results in Figure 8, a model of 6683 finite elements having 39291 DOF was chosen for the adequate modelling of the experimental vehicle. This model is shown in Figure 9 and for comparison purposes, Table 1 lists the values of the modal frequencies predicted by the nominal finite element model. Comparing with the identified modal

frequency values it can be seen that the nominal FEM-based modal frequencies for the solid element model, are closer to the experimental ones than the values for the modal frequencies predicted by the beam model. Representative modeshapes predicted by the finite solid element model are also shown in Figure 5 for the first six modes.

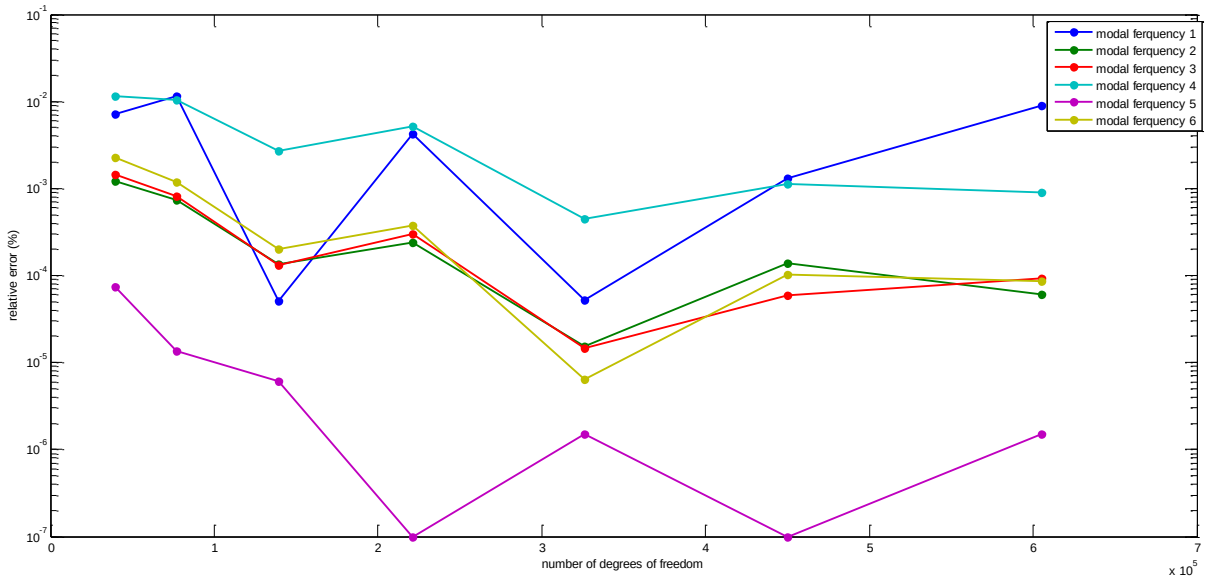

Figure 8. Relative error of the modal frequencies predicted by the finite element models with respect to the models' number of degrees of freedom.

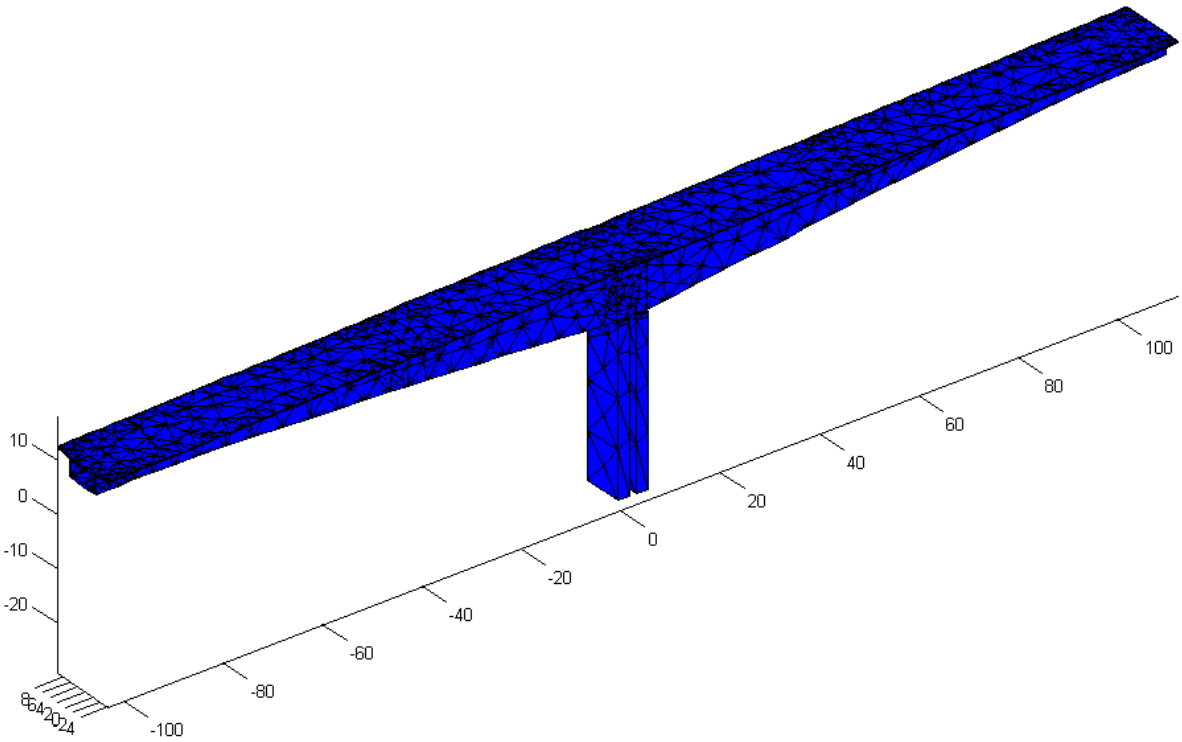

Figure 9. Finite element model of Metsovo bridge consisted of 6683 three dimensional tetrahedron elements.

The two finite element models of Metsovo bridge were employed in order to demonstrate the applicability of the proposed finite element model updating methodologies, and point out issues associated with the multi-objective identification. Both models were parameterized using three parameters. The parameterization is shown in Figure 10. The first parameter θ_1 accounts for the modulus of elasticity of the deck of the bridge, the second parameter θ_2 accounts for the modulus of elasticity of the head of the pier M3 of the bridge, while the third parameter θ_3 accounts for the modulus of elasticity of the pier M3 of the bridge. The nominal finite element model corresponds to values of $\theta_1=\theta_2=\theta_3=1$. The parameterized finite element model classes are updated using lowest five modal frequencies and modeshapes (modes 1 to 5 in Table 1) obtained from the modal analysis, and the two modal groups with modal residuals given by (2).

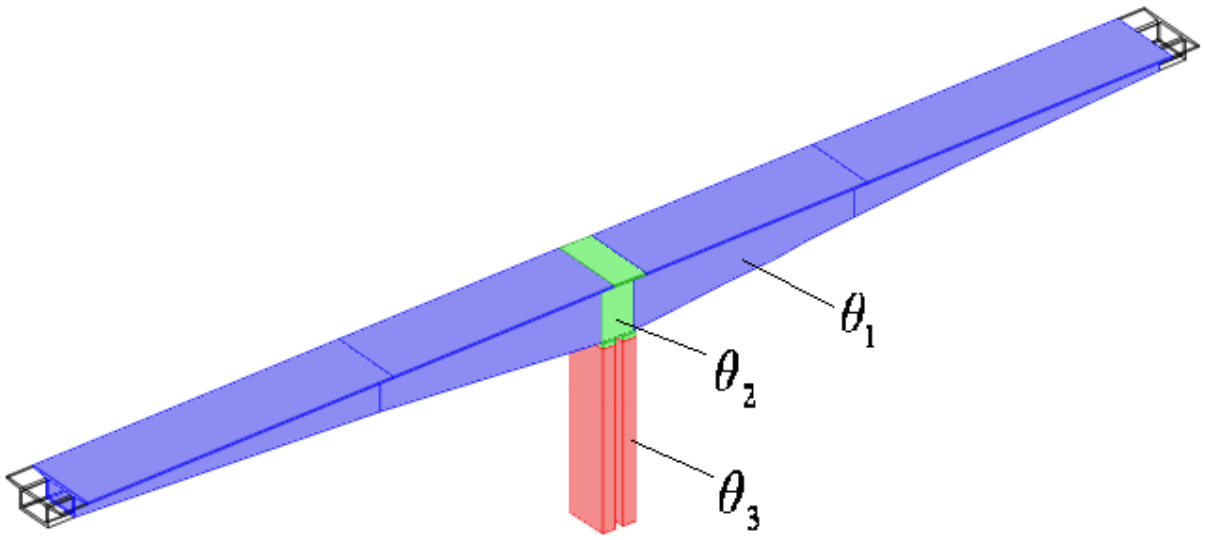

Figure 10: Parameterization of finite element model classes of Metsovo bridge.

The results from the multi-objective identification methodology for both beam and solid element models are shown in Figure 11. The normal boundary intersection algorithm was used to estimate the Pareto solutions. For each model class and associated structural configuration, the Pareto front, giving the Pareto solutions in the two-dimensional objective space, is shown in Figure 11(a). The non-zero size of the Pareto front and the non-zero distance of the Pareto front from the origin are due to modeling and measurement errors. Specifically, the distance of the Pareto points along the Pareto front from the origin is an indication of the size of the overall measurement and modeling error. The size of the Pareto front depends on the size of the model error and the sensitivity of the modal properties to the parameter values $\underline{\theta}$ [18]. Figures 11(b-d) show the corresponding Pareto optimal solutions in the three-dimensional parameter space. Specifically, these figures show the projection of the Pareto solutions in the two-dimensional parameter spaces (θ_1,θ_2), (θ_1,θ_3) and (θ_2,θ_3). It should be noted that the equally weighted solution is also computed and is shown in Figure 11.

The optimal structural models corresponding to the equally weighted (EWM) residuals methods for the beam and the solid finite element model classes are also shown in Figure 9. It can be seen that these optimal models are points along the Pareto front, as it should be expected.

It is observed that a wide variety of Pareto optimal solutions are obtained for different structural configurations that are consistent with the measured data and the objective functions used. The Pareto optimal solutions are concentrated along a one-dimensional manifold in the three-dimensional parameter space. Comparing the Pareto optimal solutions, it can be said that there is no Pareto solution that improves the fit in both modal groups simultaneously. Thus, all Pareto solutions correspond to acceptable compromise structural models trading-off the fit in the modal frequencies involved in the first modal group with the fit in the modeshape components involved in the second modal groups.

Comparing the two different element models, the solid element model seems to be able to fit better to the experimental results and this is shown in Figure 11(a). Specifically, for the higher fidelity model class of 6683 solid elements, the Pareto front moves closer to the origin of the objective space. In addition it is observed that the sizes of the Pareto fronts for the solid elements model classes reduce to approximately half the sizes of the Pareto fronts observed for the beam element model class. These results certify, as it should be expected based on the modeling assumptions, that the solid element model classes of 39291 DOF are higher fidelity model classes than the beam model classes of 306 DOF. Also the results in Figure 11(a) quantify the quality of fit, acceptance and degree of accuracy of a model class in relation to another model class based on the measure data.

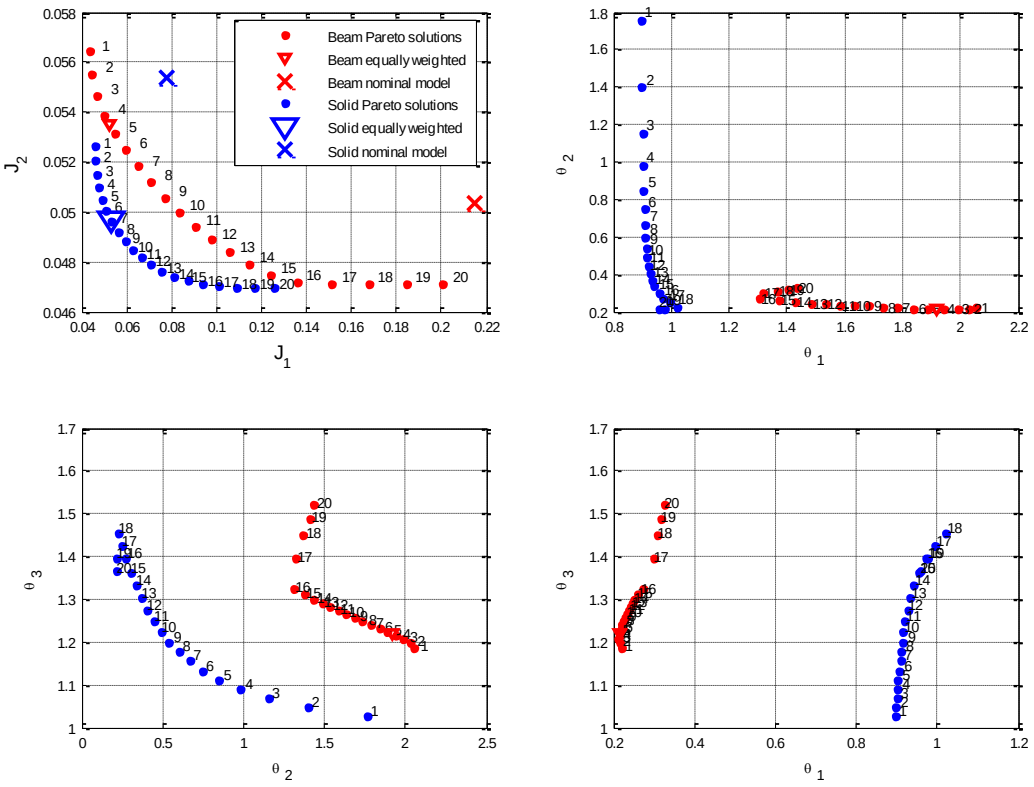

Figure 9: Pareto front and Pareto optimal solutions for the three parameter model classes in the (a) objective space and (b-d) parameter space.

The variability in the values of the model parameters for the beam element model class are of the order of 75%, 60% and 10% for θ_1, θ_2 and θ_3 respectively. It should be noted that the Pareto solutions 16 to 20 form a one dimensional solution manifold in the parameter space that correspond to the non-identifiable solutions obtained by minimizing the second objective

function. The reason for such solutions to appear in the Pareto optimal set has been discussed in reference [10]. The variability in the values of the model parameters for the solid element model class are of the order of 12%, 155% and 43% for θ_1, θ_2 and θ_3 respectively. From the results in Figure 9(b-d) one should also observe that the Pareto optimal values of the parameters predicted by the solid finite element model class are significant different from the Pareto optimal values predicted by the simpler beam finite element model class. Thus, the model updating results and parameter estimates depend highly on the fidelity of the model class considered.

The percentage error between the experimental (identified) values of the modal frequencies and the values of the modal frequencies predicted by the three parameters beam element model for the nominal values of the parameters, the equally weighted solution and the Pareto optimal solutions 1, 5, 10, 15 and 20 are reported in Table 2. Table 3 reports the MAC values between the model predicted and the experimental modeshapes for the nominal, the equally weighted and the Pareto optimal models 1, 5, 10, 15 and 20. It is observed that for the modal frequencies the difference between the experimental values and the values predicted by the Pareto optimal model vary between 0.2% and 13.4%. Specifically, for the Pareto solution 1 that corresponds to the one that minimizes the errors in the modal frequencies (first objective function), the modal frequency errors vary from 0.2% to 3.9%. Higher modal frequency errors are observed as one moves towards Pareto solution 20 since such solutions are based more on minimizing the errors in the modeshapes than the error in the modal frequencies. However, these errors from the Pareto solutions are significantly smaller than the errors observed for the nominal model which are as high as 20.1%. The MAC values between the experimental modeshapes and the modeshapes predicted by the Pareto optimal model are very close to one because of the small number of measured DOF available. The MAC values vary between 0.95 and 0.99. For the Pareto solution 20, the lowest MAC value is approximately 0.99.

For the three parameters solid element model, the percentage error between the experimental values of the modal frequencies and the values of the modal frequencies predicted by the three parameter solid element model for the nominal values of the parameters, the equally weighted solution and the Pareto optimal solutions 1, 5, 10, 15 and 20 are reported in Table 4. Table 5 reports the MAC values between the model predicted and the experimental modeshapes for the nominal, the equally weighted and the Pareto optimal models 1, 5, 10, 15 and 20. It is observed that for the modal frequencies the difference between the experimental values and the values predicted by the Pareto optimal model vary between 0.2% and 9.2%. Specifically, for the Pareto solution 1 that corresponds to the one that minimizes the errors in the modal frequencies (first objective function), the modal frequency errors vary from 0.2% to 2.9%. The range of variability of these errors is smaller than the range of variability of the errors observed from the beam model class. Higher modal frequency errors are observed as one moves towards Pareto solution 20 since such solutions are based more on minimizing the errors in the modeshapes than the error in the modal frequencies. The MAC values between the experimental modeshapes and the modeshapes predicted by the Pareto optimal model are very close to one because of the small number of measured DOF available. The MAC values vary between 0.94 and 1.

Comparing the results in the Tables 2 to 5 and the Figure 9 between the two model classes, it is evident that the Pareto optimal models from the solid element model class give better fit to the measured data than the fit provided by the beam element model class. This verifies that higher fidelity model classes tend to involve less model error and provide better fit to the measured quantities.

Mode	Relative frequency error (%)						
	Nominal model	Equally weighted	Pareto solution 1	5	10	15	20
1	-8.26	-2.86	-3.94	-2.71	-1.15	0.67	8.57
2	-7.76	3.11	2.05	3.22	4.19	5.14	12.66
3	-6.27	1.44	1.89	1.42	1.05	0.05	6.37
4	-10.15	1.14	0.20	1.22	1.97	2.66	9.88
5	-20.10	-3.70	-0.80	-4.09	-8.29	-13.45	-10.13

Table 2: Relative error between experimental and beam model predicted modal frequencies.

Mode	MAC value						
	Nominal model	Equally weighted	Pareto solution 1	5	10	15	20
1	0.996	0.998	0.997	0.997	0.997	0.997	0.997
2	0.996	0.995	0.994	0.995	0.995	0.996	0.996
3	0.955	0.959	0.952	0.960	0.966	0.973	0.976
4	0.992	0.991	0.989	0.991	0.991	0.988	0.985
5	0.985	0.973	0.973	0.973	0.976	0.978	0.979

Table 3: MAC values between experimental and beam model predicted modeshapes.

Mode	Relative frequency error (%)						
	Nominal model	Equally weighted	Pareto solution 1	5	10	15	20
1	0.11	4.41	2.88	3.89	5.53	7.65	5.38
2	-4.21	-1.80	-1.47	-1.63	-2.29	-4.00	-9.16
3	-2.71	-3.25	-3.61	-3.31	-3.24	-3.29	-6.34
4	-3.06	-0.83	-0.16	-0.64	-1.24	-2.42	-6.99
5	6.28	0.60	1.68	0.93	0.02	-0.30	-2.65

Table 4: Relative error between experimental and solid model predicted modal frequencies.

Mode	MAC value						
	Nominal model	Equally weighted	Pareto solution 1	5	10	15	20
1	0.984	0.985	0.984	0.985	0.985	0.985	0.985
2	0.997	0.998	0.997	0.998	0.998	0.999	0.999
3	0.934	0.951	0.943	0.949	0.954	0.959	0.961
4	0.999	0.999	0.999	0.999	0.999	0.998	0.997
5	0.993	0.993	0.992	0.993	0.993	0.993	0.993

Table 5: MAC values between experimental and solid model predicted modeshapes.

5 CONCLUSIONS

Methods for modal identification and structural model updating were used to develop high fidelity finite element models of the Metsovo bridge using ambient acceleration measurements. A multi-objective structural identification method was used for estimating the parameters of the finite element structural models based on minimizing two groups of modal residuals, one associated with the modal frequencies and the other with the modeshapes. The construction of high fidelity models consistent with the data depends on the assumptions made to build the mathematical model, the finite elements selected to model the different parts of the structure, the dicretization scheme controlling the size of the finite elements, as well as the parameterization scheme used to define the number and type of parameters to be updated by the methodology. The fidelity of two different model classes was examined: a simple model class consisting of a relatively small number of beam elements and a higher fidelity model class consisting of a large number of solid elements. The multi-objective identification method resulted in multiple Pareto optimal structural models that are consistent with the measured (identified) modal data and the two groups of modal residuals used to measure the discrepancies between the measured modal values and the modal values predicted by the model. A wide variety of Pareto optimal structural models was obtained that trade off the fit in various measured modal quantities. These Pareto optimal models are due to uncertainties arising from model and measurement errors. The size of observed variations in the Pareto optimal solutions depends on the information contained in the measured data, as well as the size of model and measurement errors. It has been demonstrated that higher fidelity model classes, tend to involve less model error, move the Pareto front towards the origin and reduce the size of the Pareto front in the objective space, reduce the variability of the Pareto optimal solutions, provide better fit to the measured quantities, and give much better predictions corresponding to reduced variability.

ACKNOWLEDGEMENTS

This research was co-funded 75% from the European Union (European Social Fund), 25% from the Greek Ministry of Development (General Secretariat of Research and Technology) and from the private sector, in the context of measure 8.3 of the Operational Program Competitiveness (3rd Community Support Framework Program) under grant 03-ΕΔ-524 (PENED 2003). This support is gratefully acknowledged.

REFERENCES

[1] C. Papadimitriou, J.L. Beck, L.S. Katafygiotis, Updating robust reliability using structural test data. *Probabilistic Engineering Mechanics*, **16**, 103-113, 2001.

[2] C.P. Fritzen, D. Jennewein, T. Kiefer, Damage detection based on model updating methods. Mechanical Systems and Signal Processing, **12** (1), 163-186, 1998.

[3] A. Teughels, G. De Roeck, Damage detection and parameter identification by finite element model updating. Archives of Computational Methods in Engineering, **12** (2), 123-164, 2005.

[4] M.W. Vanik, J.L. Beck, S.K. Au, Bayesian probabilistic approach to structural health monitoring. *Journal of Engineering Mechanics (ASCE)*, **126**, 738-745, 2000.

[5] E. Ntotsios, C. Papadimitriou, P. Panetsos, G. Karaiskos, K. Perros, Ph. Perdikaris, Bridge health monitoring system based on vibration measurements. *Bulletin of Earthquake Engineerin*g, doi: 10.1007/s10518-008-9067-4, 2008.

[6] K.V. Yuen, J.L. Beck, Reliability-based robust control for uncertain dynamical systems using feedback of incomplete noisy response measurements. *Earthquake Engineering and Structural Dynamics*, **32 (**5), 751-770, 2003.

[7] J.L. Beck, L.S. Katafygiotis, Updating models and their uncertainties- I: Bayesian statistical framework. *Journal of Engineering Mechanics (ASCE)*, **124 (**4), 455-461, 1998.

[8] Y. Haralampidis, C. Papadimitriou, M. Pavlidou, Multi-objective framework for structural model identification. *Earthquake Engineering and Structural Dynamics*, **34** (6), 665-685, 2005.

[9] K. Christodoulou, C. Papadimitriou, Structural identification based on optimally weighted modal residuals. *Mechanical Systems and Signal Processing*, **21**, 4-23, 2007.

[10] K. Christodoulou, E. Ntotsios, C. Papadimitriou, P. Panetsos, Structural model updating and prediction variability using Pareto optimal models. *Computer Methods in Applied Mechanics and Engineering*, **198** (1), 138-149, 2008.

[11] E. Ntotsios, C. Papadimitriou, Multi-objective optimization algorithms for finite element model updating. *International Conference on Noise and Vibration Engineering (ISMA2008)*, Katholieke Universiteit Leuven, Leuven, Belgium, September 15-17, 2008.

[12] R.B. Nelson, Simplified calculation of eigenvector derivatives. *AIAA Journal*, **14** (9), 1201-1205, 1976

[13] A. Teughels, G. De Roeck, J.A.K. Suykens, Global optimization by coupled local minimizers and its application to FE model updating. *Computers and Structures*, **81** (24-25), 2337-2351, 2003.

[14] H. G. Beyer, *The theory of evolution strategies*, Berlin, Springer-Verlag, 2001.

[15] E. Zitzler, L. Thiele, Multi-objective evolutionary algorithms: A comparative case study and the strength Pareto approach. *IEEE Transactions on Evolutionary Computation*, **3**, 257-271, 1999.

[16] I. Das, J.E. Jr. Dennis, Normal-Boundary Intersection: A new method for generating the Pareto surface in nonlinear multi-criteria optimization problems. *SIAM Journal of Optimization*, **8**, 631-657, 1998.

[17] E. Ntotsios, C. Papadimitriou, Multi-objective optimization framework for finite element model updating and response prediction variability. *Inaugural International Conference of the Engineering Mechanics Institute (EM08)*, Department of Civil Engineering University of Minnesota, Minneapolis, Minnesota, May 18-21, 2008.

[18] E. Ntotsios, Experimental modal analysis using ambient and earthquake vibrations: Theory, Software and Applications. MS Thesis Report No. SDL-09-1, Department of Mechanical and Industrial Engineering, University of Thessaly, Volos, 2008.

[19] COMSOL AB, *COMSOL Multiphysics user's guide*, 2005, [http://www.comsol.com/].